

# Dynamic Changes in Vegetation and Driving Mechanisms at the Northern Edge of the Kubuqi Desert

Ping MIAO<sup>1</sup>, Rongyang WANG<sup>2</sup>, Ziyuan QIN<sup>2\*</sup>, Hexiang ZHENG<sup>2</sup>, Hongli MA<sup>1</sup>, Jun WANG<sup>2</sup>, Haofang YAN<sup>3</sup>

1. River and Lake Protection Center of Ordos City, Ordos 017000, China; 2. Pastoral Water Conservancy Science Research Institute of the Ministry of Water Resources, Hohhot 010020, China; 3. Research Center of Fluid Machinery Engineering and Technology, Jiangsu University, Zhenjiang 212013, China

**Abstract** Based on multi-source time-series data from 2017 to 2024, this study comprehensively employed Theil-Sen trend analysis, Mann-Kendall test, random forest regression model, and spatial and temporal lag correlation analysis to systematically investigate the variation characteristics of NDVI and their associated mechanisms with land use changes and groundwater depth in the study area. The results indicate that vegetation activity showed overall significant improvement during the study period, with 60.93% of the area exhibiting significant greening trends and only 6.55% showing degradation. The trajectory characteristics of land use changes could explain approximately 79.64% of the variation in NDVI trends, but their driving effects demonstrated significant spatial heterogeneity, with core driving zones accounting for 79.22% of the area. Groundwater depth showed an overall weak negative correlation with NDVI ( $r = -0.0464$ ), but exhibited significant lag effects, and the correlation coefficient increased to  $-0.1763$  when there was a lag of 3 months. The study concludes that regional vegetation changes were primarily driven by land use activities, while the influences of groundwater showed spatial and temporal lag characteristics. Ecological restoration policies should integrate land use optimization with water resource management, and fully consider the spatial heterogeneity and temporal lag effects of driving mechanisms.

**Key words** Kubuqi Desert; NDVI; Groundwater depth; Theil-Sen trend analysis; Land use change

**DOI** 10.19547/j.issn2152-3940.2026.01.001

The Kubuqi Desert is the seventh largest desert in China<sup>[1]</sup>, with an area of approximately 18 600 km<sup>2</sup>. The desert vegetation ecosystem is more sensitive to environmental change<sup>[2]</sup>, so revealing the dynamic evolution patterns of vegetation coverage and driving mechanisms is of great significance for understanding the impact of climate change and human activities on the ecosystem, as well as improving the management of vegetation resources and desert governance<sup>[3-4]</sup>. Due to strong applicability and ease of acquisition, normalized difference vegetation index (NDVI)<sup>[5]</sup> has become one of the commonly used indicators for characterizing vegetation changes at home and abroad, and is currently the core preferred indicator for analyzing the vegetation coverage, growth dynamics, and long-term trends of deserts<sup>[6-8]</sup>.

In the dynamic monitoring of desert vegetation coverage, slope trend analysis is the core method for quantifying long-term change patterns. Current mainstream methods include linear regression<sup>[9]</sup>, moving average method<sup>[10-12]</sup>, Sen slope method, and the accompanying Mann-Kendall (MK) test method<sup>[13-14]</sup>. In the analysis of the dynamic trend of desert vegetation coverage, the linear regression method has obvious limitations due to its reliance on normal distribution and weak ability to handle outliers, while the moving average method has distinct limitations because of its inability to quantify the slope and high subjective interference. The combination of Sen slope and MK test has become the pre-

ferred method in this field due to its adaptability to non-normal data, robustness in handling outliers, adaptability to long-time series, and the integration of "quantification + testing". It has been extensively documented that the results are significantly more consistent with the actual ecological processes than those obtained through other methods. Land use type is an important factor affecting the vegetation changes in the Kubuqi Desert, but a single linear method is unable to capture the nonlinear relationship between land use trajectory and NDVI<sup>[15]</sup>. To further explore the correlation between land use change trajectory and NDVI trend, multiple analysis methods, including linear regression, single decision tree, and random forest, were compared. Finally, the random forest model was chosen, and the deep-level correlation between land use changes and NDVI trends were explored based on its ability to depict complex nonlinear relationships and the advantages of ensemble learning.

Groundwater, as an important component of terrestrial ecosystems, plays a crucial role in maintaining ecosystems in arid regions. Zhang Xiaoyu *et al.*<sup>[16]</sup> studied the relationship between the characteristics of plant communities in the ecosystem and the ecological threshold of groundwater depth, and concluded that an appropriate groundwater depth can promote the growth and development of plant communities in arid regions. Zhang Jingyu<sup>[17]</sup> explored the temporal and spatial variability of groundwater level and vegetation index (NDVI) in the Hebei Plain, and found that groundwater depth was significantly negatively correlated with NDVI. The core objective of this study is to use the Pearson correlation coefficient method<sup>[18]</sup> to measure the linear correlation between NDVI and groundwater depth, and systematically analyze

Received: November 16, 2025 Accepted: December 18, 2025

Supported by the Key Special Project for Water Conservancy Science and Technology of Ordos City (ESKJ2023-001).

\* Corresponding author.

the quantitative relationship between vegetation growth status (represented by NDVI) and groundwater supply (represented by depth) and its temporal-spatial patterns. Precisely matching the ecological correlation characteristics of "NDVI-groundwater depth" (linear in the appropriate range, and non-linear in the threshold range) not only addresses the limitations of a single coefficient but also distinguishes the type of correlation through the "significance" of the two coefficients.

In this paper, the long-term change trends of NDVI in the northern edge area of the Kubuqi Desert were studied, and the temporal and spatial change patterns of the correlation between changes in land use types and NDVI were analyzed. At the same time, by comparing the measured data of water level with changes in NDVI in a short period (13 months), the lag effect in time and space was discussed, and their correlation was discussed. This study aims to provide a scientific basis for the restoration of ecosystems and water resource management in arid and semi-arid regions.

## 1 Materials and methods

**1.1 General situation of the study area** The study area ( $40^{\circ}36'4'' - 40^{\circ}43'44''$  N,  $107^{\circ}30'24'' - 107^{\circ}43'19''$  E) is located in the northwest of Hangjin Banner, Ordos City, Inner Mongolia Autonomous Region (Fig. 1), and is adjacent to the irrigation area on the south bank of the Yellow River in Hangjin County. The shortest straight-line distance from the Yellow River is 3.3 km. It is 18.15 km long from east to west and 14.20 km wide from north to south, with a total area of 90.95 km<sup>2</sup>. The study area has a mid-temperate continental climate, with little rainfall, intense evaporation and abundant sunlight. Due to differences in landform, climate, vegetation, and water conditions, the types of soil in Hengjin County show distinct regional differentiation patterns: saline-alkali soil, sandy soil, and grassland soil are distributed successively from north to south; from east to west, there are loamy calcareous soil, brown calcareous soil, gray desert soil, and brown desert soil. The Kubuqi Desert is dominated by sandy soil, which is loose in structure, poorly differentiated, and poor in nutrients, making it unsuitable for farming. The soil in the study area is mainly loam, of which silty sandy loam and sandy loam are widely distributed. The main vegetation is reeds, creeping grass, *Artemisia desertorum* Spreng., and so forth.

**1.2 Sources of data** The data of NDVI, land use, *etc.* were sourced from the platform Google Earth Engine (GEE). The data of groundwater depth were the actual measurement data from the HOBO self-measuring water level gauge, and it was automatically recorded every 3 h. To ensure the application of the three sets of data in Python, bilinear interpolation smoothing processing was carried out on the data of NDVI and groundwater depth by using resampling technology, so as to ensure the consistency of the data. The spatial distribution of groundwater depth, annual average NDVI, and the mean NDVI of the designated month in the study area in 2022 is shown in Fig. 2 and Fig. 3. The data of NDVI are divided into two parts: the monthly data between 2017 and 2024

(for analyzing the changing trends), and the monthly data from July 2021 to July 2022 (for studying the short-term relationship with groundwater depth). As shown in the spatial distribution of the annual average NDVI from 2017 to 2024 and the monthly average NDVI from July 2021 to July 2022 in the study area (Fig. 3), NDVI was below 0.4 in most areas, and the minimum was  $-0.3$ , while it was relatively low in the east and north. From Fig. 2, it can be seen that groundwater depth was generally between 1 and 3 m, and there was no significant variation between seasons. There were some overall obvious rises and drops in the seasons. Fig. 4 shows that land use types changed significantly between 2017 and 2022, and large areas of bare soil was transformed into water body and bushes.

### 1.3 Research methods

**1.3.1 NDVI.** NDVI can reflect the growth status of vegetation on the underlying surface. It can be calculated by using the reflectivity in the near-infrared band and the red light band of Landsat images, and its range is  $NDVI \in [-1.0, 1.0]$ . The formula is as follows:

$$NDVI = \frac{\rho_{NIR} - \rho_{RED}}{\rho_{NIR} + \rho_{RED}} \quad (1)$$

$$NDVI_i = \text{Max} (NDVI_{ij}) \quad (2)$$

Formula (1) was first proposed and systematically elaborated by Rouse *et al.*<sup>[19]</sup> in their research on the Landsat satellite (then known as ERTS). Formula (2), the maximum value compositing (MVC), was proposed by Holben<sup>[20]</sup>. It is used to generate a high-quality synthetic image that is least affected by clouds and the atmosphere from multiple NDVI images over a period of time (such as one month).

**1.3.2 Analysis system of NDVI trends.**

**1.3.2.1 Time series decomposition**—STL (seasonal-trend decomposition using LOESS). STL, a robust time series decomposition method, was fully proposed and described by Cleveland<sup>[21]</sup>. It is insensitive to outliers, and can flexibly handle nonlinear trends and changing seasonal cycles, so it is highly suitable for analyzing time series of NDVI. In this paper, the data of NDVI from 2017 to 2023 were decomposed into three components: trend component (long-term change pattern), seasonal component (periodic fluctuations), residual component (random fluctuations). The period was also fixed (12 months), that is, the data were the monthly data in 12 months per year. The formula of STL is as follows:

$$Y_t = T_t + S_t + R_t \quad (3)$$

In the formula,  $Y_t$  is the observation value of NDVI at time  $t$ ;  $T_t$  is trend component;  $S_t$  is seasonal component;  $R_t$  is residual component.

**1.3.2.2 Trend estimation**—Theil-Sen slope estimation. Vegetation changes are typically slow processes. Theil-Sen slope estimation was proposed by Theil<sup>[13]</sup> and extended and refined by Sen<sup>[22]</sup>. In the detection of remote sensing change, the traditional ordinary least squares (OLS) fits the trend by minimizing the squared error, which is susceptible to the influence of extreme values. Theil-Sen, by calculating the median slope of all time point

pairs ( $n(n-1)/2$  combinations), can more stably capture weak but persistent long-term trends, avoiding the interference of short-term climate events.

$$\beta = \text{median}\left(\frac{y_j - y_i}{x_j - x_i}\right) \quad i < j \quad (4)$$

$\beta > 0$  indicates that there is an increase in NDVI, suggesting a significant improvement in vegetation. Conversely,  $\beta < 0$  means NDVI decreases, which indicates environmental degradation and might signify desertification.

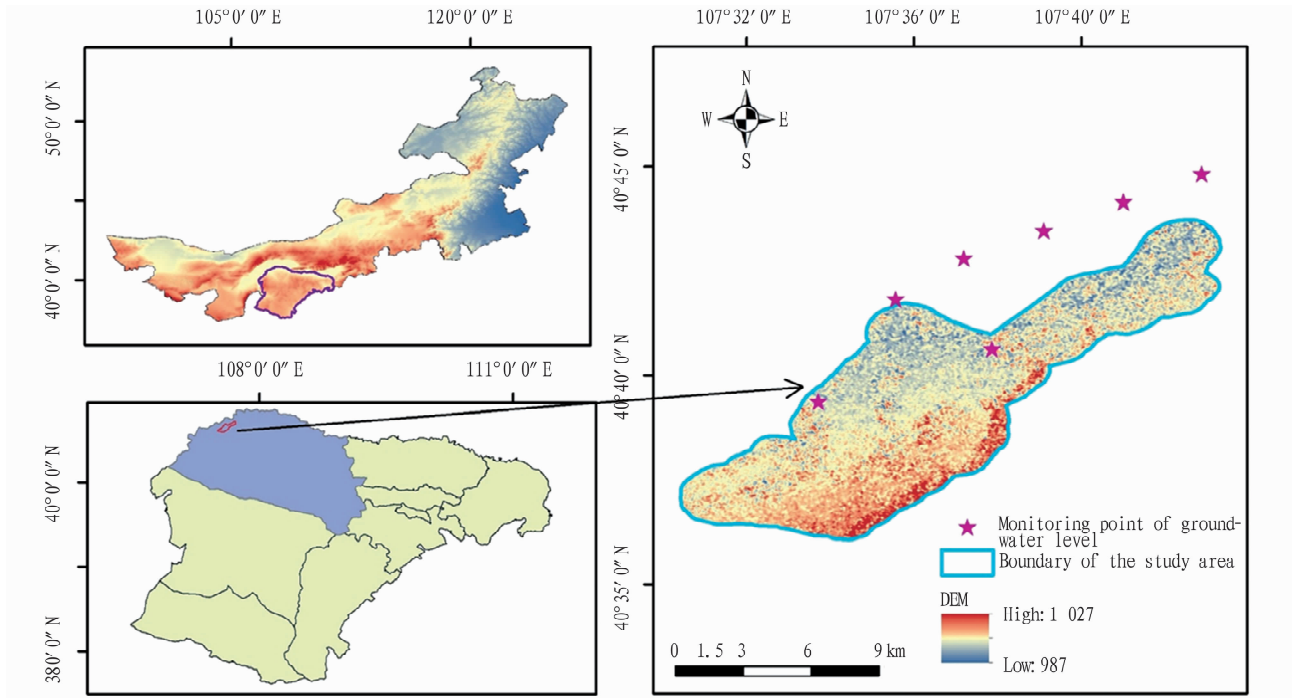
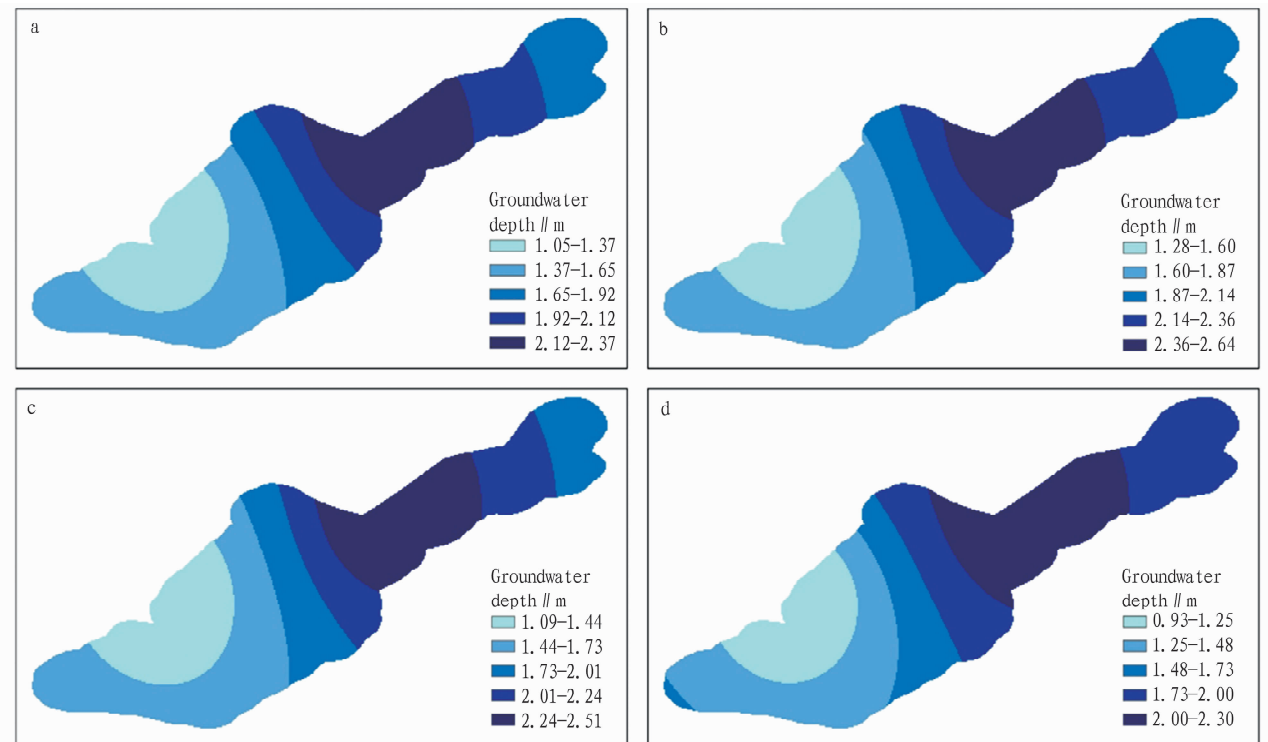


Fig. 1 Location and elevation map of the experimental area



Note: a. Spring; b. Summer; c. Autumn; d. Winter.

Fig. 2 Groundwater depth of the study area in 2022

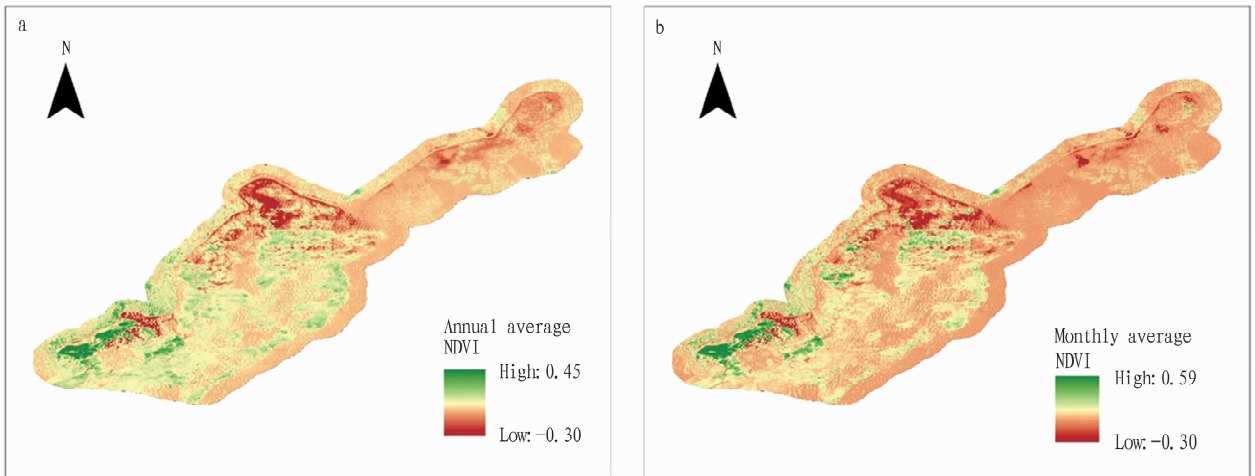


Fig.3 Annual average NDVI (a) and the mean NDVI of the designated month (b) in 2022

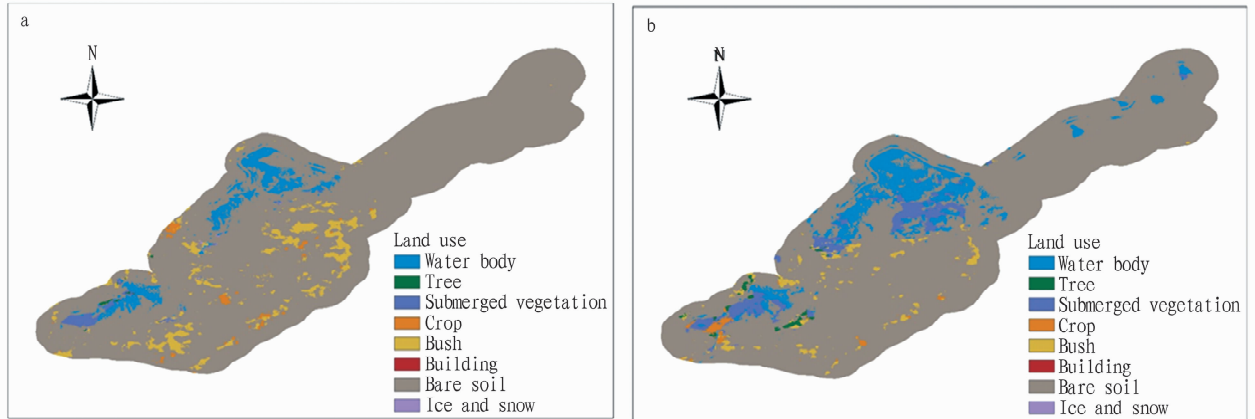


Fig.4 Maps of land use in 2017 (a) and 2022 (b)

**1.3.2.3 Trend significance test—Mann-Kendall test.** Mann-Kendall test, a non-parametric trend testing method, was developed by Mann<sup>[23]</sup> and Kendall. In research on ecological remote sensing, the combination of Theil-Sen slope estimation and Mann-Kendall significance test has become a standard paradigm for analyzing long-term trends of vegetation dynamics, often referred to as the "Sen + MK" method, and is widely applied in studies on vegetation change at regional and even global scales. MK solution: distinguishing trends through statistical tests ( $p$  value). Significant trend ( $p < 0.05$ ): vegetation continues to deteriorate/recover; non-significant change: short-term fluctuations (no need for intervention).

Test statistic ( $S$ ) can be calculated as follows:

$$S = \sum_{i=1}^{n-1} \sum_{j=i+1}^n \text{sgn}(y_j - y_i) \quad (5)$$

$$\text{sgn}(z) = \begin{cases} 1 & z > 0 \\ 0 & z = 0 \\ -1 & z < 0 \end{cases} \quad (6)$$

$S > 0$  indicates an upward trend, while  $S < 0$  means a downward trend.

The significance of change trends can be determined based on  $Z$  and  $p$  values, and  $Z$  can be calculated as follows:

$$Z = \begin{cases} \frac{S-1}{\sqrt{\text{Var}(S)}} & S > 0 \\ 0 & S = 0 \\ \frac{S+1}{\sqrt{\text{Var}(S)}} & S < 0 \end{cases} \quad (7)$$

$|Z| > 1.96 \rightarrow p < 0.05$  means a significant trend, and  $|Z| > 2.58 \rightarrow p < 0.01$  stands for an extremely significant trend.

**1.3.3 Analysis of the correlation between NDVI and land use.** Machine learning and spatial analysis were combined to explore the mechanism of the relationship between the trajectory of land use changes and the trend of NDVI. The core framework is as follows: based on the research paradigm of "feature extraction – model construction – validation and interpretation", a predictive model between land use changes and the trend of NDVI was established by quantify the characteristics of land use changes, and the intrinsic correlation was revealed through statistical verification and spatial analysis. The prediction model for the trend of NDVI is the one applied in section 3.2.

**1.3.3.1 Extraction of trajectory features of land use changes.** Pixel-level time series features (such as change frequency, initial/terminal land use type, stability, etc.) was extracted, and entropy was used to measure the complexity of a change. Stability

indicator was used to quantify the frequency of the change, and then trajectory ID encoding was conducted to extract change features from the time series.

The number of changes  $C$  can be calculated as follows:

$$C = \sum_{i=1}^{n-1} I(LU_i \neq LU_{i+1}) \quad (8)$$

In the formula,  $I(\cdot)$  is the indicator function;  $LU_i$  represents the land use type in the  $i^{\text{th}}$  year;  $n$  is the total number of years.

The formula of stability  $S$  is as follows:

$$S = \frac{\max_k(N_k)}{n} \quad (9)$$

In the formula,  $N_k$  is the frequency of type  $k$ .

Change entropy  $H$  is as follows:

$$H = - \sum_{k=0}^8 p_k \log(p_k) \quad (10)$$

In the formula,  $p_k$  represents the probability of type  $k$ . The entropy was used to measure the complexity of a change. The higher the entropy is, the more irregular the change is.

The frequency of changes is as follows:

$$F = \frac{C}{n-1} \quad (11)$$

$F$  represents the intensity of changes within a unit of time.

**1.3.3.2 Modeling and prediction.** In this paper, in order to construct a correlation model between land use changes and NDVI trends and quantify the explanatory power of the former for the latter, the machine learning method random forest (RF) regression was selected. Random forest is a classic ensemble learning algorithm proposed by Breiman<sup>[24]</sup>. RF was used to establish the mapping relationship between the trajectory characteristics of land use changes and NDVI trends, and Rodriguez-Galiano<sup>[25]</sup> had already demonstrated the effectiveness of RF in the classification of remote sensing land cover.

By using the ensemble learning method based on multiple decision trees, multiple trees were constructed through Bootstrap sampling, and the final prediction was the average of the results of each tree, thereby reducing the risk of overfitting.

$y$  is the prediction value of NDVI trend slope  $\hat{y}$  is as follows:

$$\hat{y} = \frac{1}{M} \sum_{m=1}^M f_m(x) \quad (12)$$

In the formula,  $M$  represents the number of decision trees;  $f_m(x)$  is the prediction value of the  $m$ th tree.

**1.3.3.3 Evaluation of model performance.** To systematically evaluate the prediction performance and stability of the model and ensure the reliability of the results, performance indicators, cross-validation and residual analysis were adopted respectively.

**1.3.3.3.1 Performance indicators.** Performance indicators include three indicators used to quantify the prediction accuracy of the model, namely mean squared error (MSE), root mean squared error (RMSE), and coefficient of determination ( $R^2$ ). Their formulas are as follows:

$$MSE = \frac{1}{n} \sum_{i=1}^n (y_i - \hat{y}_i)^2 \quad (13)$$

$$RMSE = \sqrt{MSE} \quad (14)$$

$$R^2 = 1 - \frac{\sum (y_i - \hat{y}_i)^2}{\sum (y_i - \bar{y})^2} \quad (15)$$

In the formulas,  $\bar{y}$  represents the mean of observation values, with a range of  $[0, 1]$ . The closer it is to 1, the better the fit.

**1.3.3.3.2 Cross-validation.** K-fold cross-validation is a standard procedure for evaluating the generalization performance and stability of a model. It was developed and popularized by Stone<sup>[26]</sup> and Geisser<sup>[27]</sup>, and has now become the gold standard for training and validating machine learning models.

**Principle:** By splitting the training set and test set multiple times, the stability of the model is evaluated. In the code, 10-fold cross-validation (KFold) is used:

$$CV \text{ score} = \frac{1}{10} \sum_{k=1}^{10} \text{Score}(k) \quad (16)$$

In the formula,  $\text{score}(k)$  means the performance indicator for the  $k^{\text{th}}$  fold, such as  $R^2$  or RMSE.

**1.3.3.3.3 Residual analysis.** Based on prediction residual (actual value-prediction value), the deviation and error of the model can be evaluated. Absolute residual  $r_i$  and relative residual  $rr_i$  can be calculated as follows:

$$r_i = |y_i - \hat{y}_i| \quad (17)$$

$$rr_i = \frac{|y_i - \hat{y}_i|}{|y_i|} \quad (18)$$

**1.3.3.4 Spatial statistical analysis and verification.** Residual spatial distribution was used to identify strongly correlated areas, and OPTICS clustering was used to recognize different change patterns. Spatial autocorrelation analysis (using spatial coordinates as features) was conducted, and the contribution of each feature to the prediction results was finally quantified by using SHAP values. Here, SHAP (Shapley Additive Explanations), a method based on game theory, is used to explain the output of any machine learning model. It was proposed by Lundberg *et al.*<sup>[28]</sup>, and can consistently and fairly distribute the contribution of each feature to a single prediction result. In the study, SHAP values can be used to clearly reveal which land use change feature, such as "change frequency" and "stability", has the greatest impact on the trends of NDVI, significantly enhancing the interpretability of the model.

$$\arg \min_C \sum_{k=1}^K \sum_{x \in C_k} \|x - \mu_k\|^2 \quad (19)$$

$C_k$  represents the  $k^{\text{th}}$  cluster;  $\mu_k$  is the center of the cluster, and  $k=5$ .

$$\text{reach-dist}(p, o) = \max(\text{core-dist}(o), d(p, o)) \quad (20)$$

In the formula,  $\text{core-dist}(o)$  represents the core distance, and  $d(p, o)$  is the distance between two points.

SHAP values were analyzed as follows:

$$\phi_i = \sum_{s \subseteq \mathcal{F} \setminus \{i\}} \frac{|S|! (|\mathcal{F}| - |S| - 1)!}{|\mathcal{F}|!} [f(S \cup \{i\}) - f(S)] \quad (21)$$

In the formula,  $\phi_i$  is the SHAP value of feature  $i$ ;  $\mathcal{F}$  represents the entire set of features. Positive values indicate that the feature contributes to an increase in the prediction value, while negative values means the opposite conclusion.

**1.4 Analysis of the correlation between groundwater depth and NDVI** All data were unified to the WGS84 coordinate system (EPSG: 4326), and the vector boundary of the study area was used for clipping. To deeply study the correlation between groundwater depth and NDVI, the distribution map of groundwater depth in 13 months was constructed based on the measured data from July 2021 to July 2022, and the map of groundwater depth was aligned with the distribution map of NDVI over the 13 months. To eliminate the influence of units, the NDVI data have been converted to the standard range of  $-1$  to  $1$ . Finally, 749 valid sampling points were systematically generated within the study area, and a total of 9 737 pairs of valid data of NDVI and groundwater depth were obtained for analysis.

Furthermore, the Python tool and the Pearson correlation coefficient method was used to measure the linear correlation degree (positive correlation/negative correlation and intensity) between NDVI and groundwater depth. The Spearman's rank correlation coefficient was used as a comparison for quantifying the correlation degree. The formula of Pearson correlation coefficient is as follows:

$$r = \frac{\sum_{i=1}^n (x_i - \bar{x})(y_i - \bar{y})}{\sqrt{\sum_{i=1}^n (x_i - \bar{x})^2} \cdot \sqrt{\sum_{i=1}^n (y_i - \bar{y})^2}} \quad (22)$$

$\bar{x}$  and  $\bar{y}$  represent the means of  $x$  and  $y$ , respectively; the numerator is the covariance of  $x$  and  $y$  (measuring the degree of covariance); the denominator is the product of the standard deviations of the two (standardization process, making the range of  $r$   $[-1, 1]$ ). For each pixel in the image sequence,  $r$  value was calculated separately, resulting in a correlation coefficient graph, where the size and sign of  $r$  are displayed pixel by pixel.  $r > 0$  indicates a positive correlation (as the independent variable increases, the pixel value also increases);  $r < 0$  means a negative correlation (as the independent variable increases, the pixel value decreases), reflecting the direction and strength of the correlation between NDVI and groundwater depth in different areas.

Spearman's rank correlation coefficient means that the values of two variables separately are ranked, and then the Pearson correlation coefficient between the grades is calculated.

$$\rho = 1 - \frac{6 \sum d_i^2}{n(n^2 - 1)} \quad (23)$$

Coefficient  $\rho$  measures the strength of a monotonic relationship (not necessarily linearity). It is more robust than the Pearson coefficient, and is not sensitive to outliers.

**Lagged correlation:** NDVI (vegetation growth) is affected by groundwater depth, but the vegetation's response to groundwater is not immediate; after the groundwater changes, it takes some time for the vegetation to adjust its growth state (such as root water absorption and changes in photosynthesis). The analysis of lagged correlation aims to quantify this response time.

## 2 Results and analysis

**2.1 Changing trends of NDVI** Based on the time series data

of NDVI in the study area from 2017 to 2024, the changing trends of NDVI were analyzed. Overall, the NDVI in the study area showed a moderate growth trend (Fig. 5). The average of annual NDVI change slope (Theil-Sen estimation) was 0.006, indicating that vegetation coverage showed an overall improvement trend in the study period.

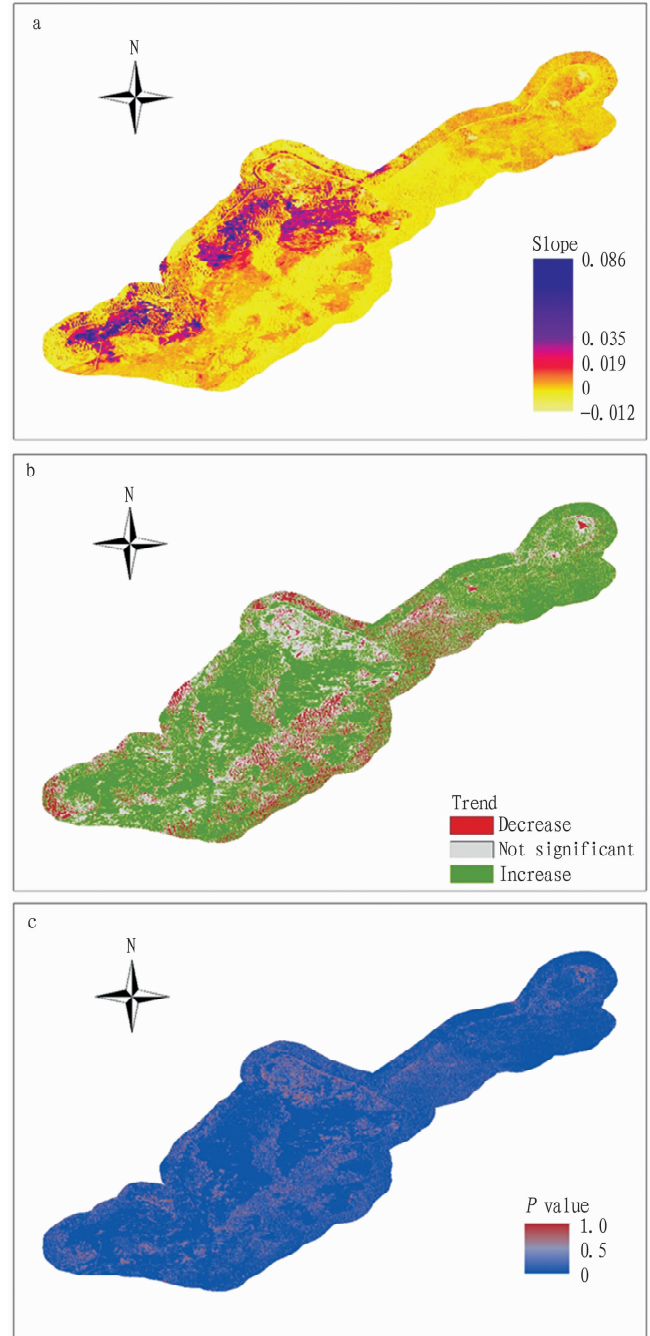


**Fig. 5** Spatial distribution of NDVI slope, trend classification, and  $P$  value

The growth trend within the study area was universal, with a median slope of 0.003, indicating that annual average growth of NDVI was not less than 0.003 in over 50% of the pixels, reflect-

ting the widespread universality of the growth trend in the study area. From the perspective of significant trends, there was a significant upward trend ( $p < 0.05$ ) in 60.93% of the pixels, which was the dominant change in the study area, indicating that vegetation was improved in most areas. From Fig. 5, it can be clearly observed that there was spatial heterogeneity in the change amplitude. The standard deviation of slope was 0.010, and the range of variation was large (from  $-0.052$  to  $0.089$ ), revealing that there were significant spatial differences in the changes of NDVI in the study area. The extreme improvement areas (slope  $> 0.05$ ) may be areas where vegetation restoration projects in recent years have achieved remarkable results, such as the construction and implementation of the floodwater diversion project. The extreme degradation areas (slope  $< -0.03$ ) may be affected by human activities (such as excessive development) or natural factors (such as drought). As shown in Fig. 6, the proportion of pixels with a significant downward trend was low, only 6.55%, indicating that degradation regions were concentrated and had a limited range. There was no significant trend in another 32.51% of the pixels, and they corresponded to regions with relatively stable ecosystems or those that have received less disturbance. In the study area, 67.56% of the pixels showed a statistically significant trend (upward + downward trend), belonging to a medium reliability level. It indicates that the overall trend had a clear signal, and driving factors should be used for analysis. Among them, the average slope rate of the areas with a significant change was up to 0.009, higher than the overall average, showing that the vegetation growth in the significantly improved areas was stronger, and the ecological effect was more prominent.

**2.2 Correlation between NDVI and land use** Based on the highly dynamic changes in environmental characteristics of the Kubuqi Desert, strict data quality control standards were adopted, and only pixels with reliable land cover classification for eight consecutive years (accounting for 35.10% of the study area) were retained. This screening criterion ensures that the trajectory analysis was based on reliable and consistent data of land use, avoiding the interference of the movement of sand dunes, mixed pixels, and classification uncertainties on the results.

To study the association mechanism between land use changes and NDVI trends, the multi-dimensional characteristics of land use change trajectories (such as the number of changes, stability, entropy, *etc.*) were extracted by loading the data of NDVI trends, land use from 2017 to 2024, and boundary of the study area. The random forest method model was used to analyze the explanatory power of these trajectory characteristics for NDVI trends. Clustering and residual analysis methods were combined to identify strongly correlated areas. Finally, spatial distribution maps, statistical results, and reports were generated to quantify the impact of land use changes on NDVI trends and reveal their driving mechanisms. The distribution of strongly correlated areas is shown in Fig. 7.

Residual average was  $-0.023432$ . Here, residual was the

difference between the actual value of NDVI trends and the model's prediction value. If the average was close to 0, the model had no systematic bias (neither overestimating nor underestimating NDVI trends overall). Therefore, the difference between the actual value of NDVI trends and the model's prediction value met the requirements, and the prediction direction was relatively reliable. Among them, the proportion of relative residual  $< 5\%$  was 6.71%. Relative residual ( $| \text{residual} | / \text{actual value}$ ) reflects the prediction accuracy. Relative residual  $< 5\%$  indicates an extremely small prediction error. Only 6.71% of the areas met this level of precision, suggesting that the trajectory of land use changes in most areas had a weak "accurate explanation ability" for NDVI trends. This might be due to the complex trajectory characteristics (such as frequent changes) or the stronger interference of NDVI by other factors.

The proportion of strongly correlated areas was 79.22%. Strongly correlated areas refer to the areas where the trajectory of land use changes was significantly associated with NDVI trends (determined by the residual threshold). This proportion indicates that in approximately 79.22% of the study areas, land use changes were the core factor driving NDVI trends. In the remaining areas, NDVI trends might be dominated by other factors (such as precipitation, temperature changes, policy interventions, *etc.*).

In Fig. 7, SHAP value is the contribution degree of a feature to the model output. Positive values indicate that the feature contributed to the increase of prediction values (making vegetation greener and growing faster), while negative values mean that the feature contributed to the decrease of prediction values (causing vegetation degradation, and slower growth).

The number of changes: blue points (low values) represent pixels where there was little or no change in land use type during 2017 – 2024. Red points (high values) stand for pixels where land use type changed multiple times during this period.

Initial class and final class: blue points (low values) mean land waters, trees, *etc.* Red points (high values) represent bare ground or buildings. In the figure, it is obviously shown that high values of bare soil are focused on the negative values of SHAP, contributing to the impact of vegetation degradation.

Dominant class: if blue points (such as forests, and grasslands) are concentrated on the right side, NDVI showed a positive growth trend in areas mainly covered by vegetation. If red points (such as bare land, and buildings) are concentrated on the left side, NDVI was negatively degraded in areas mainly covered by non-vegetation.

Longitude, latitude, row index, and column index represent the contribution of location to SHAPE, that is, various locations bring different contributions. However, due to the small undulation of the experimental area, the obtained results are generally poor, and cannot reflect the significant differences in the degree of contribution brought by different locations and different terrain conditions.

Entropy: blue points (low values) stand for a very pure land type sequence, with high order (almost always the same land

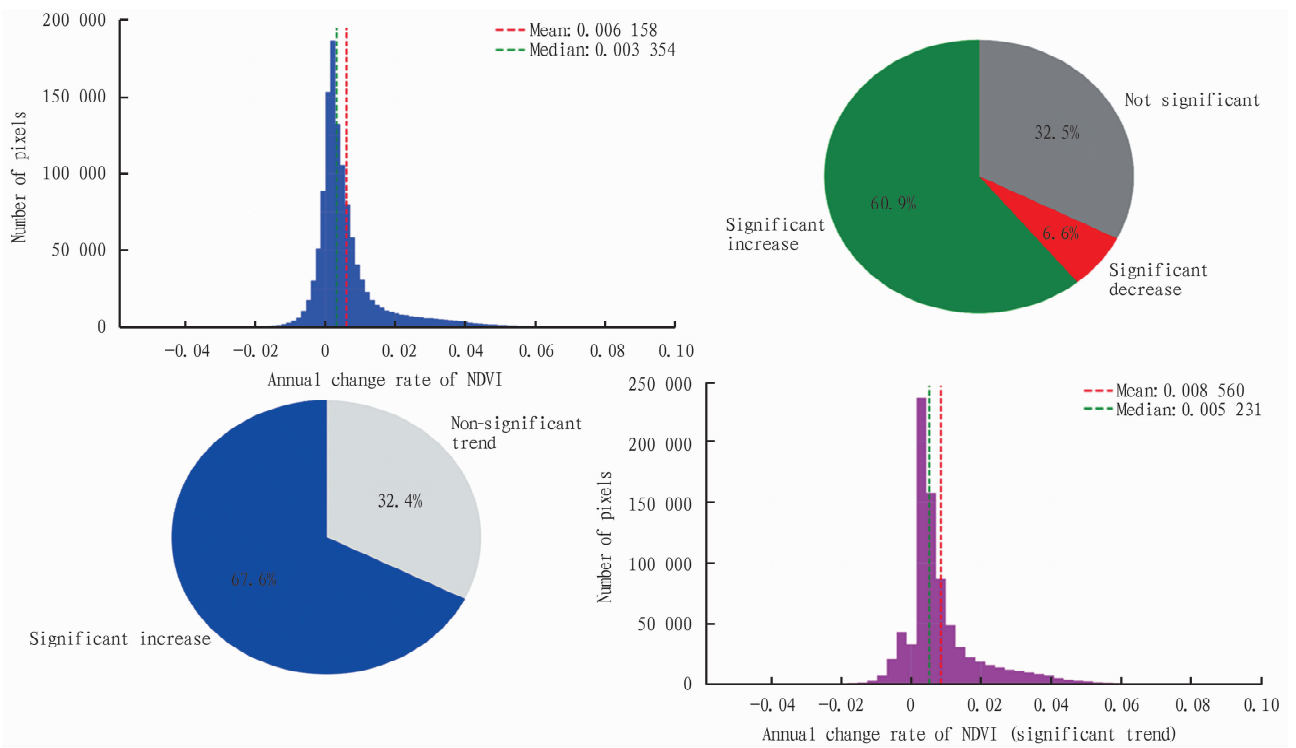


Fig.6 Statistical charts of verification results

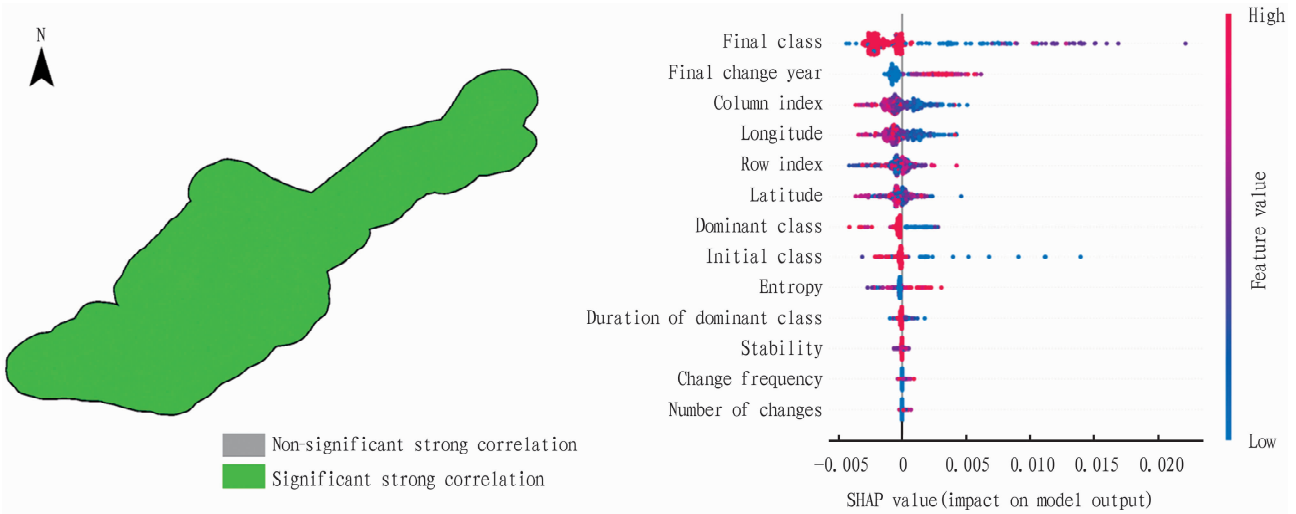


Fig.7 Distribution of areas with strong correlation between NDVI and land use and the contribution of SHAP value

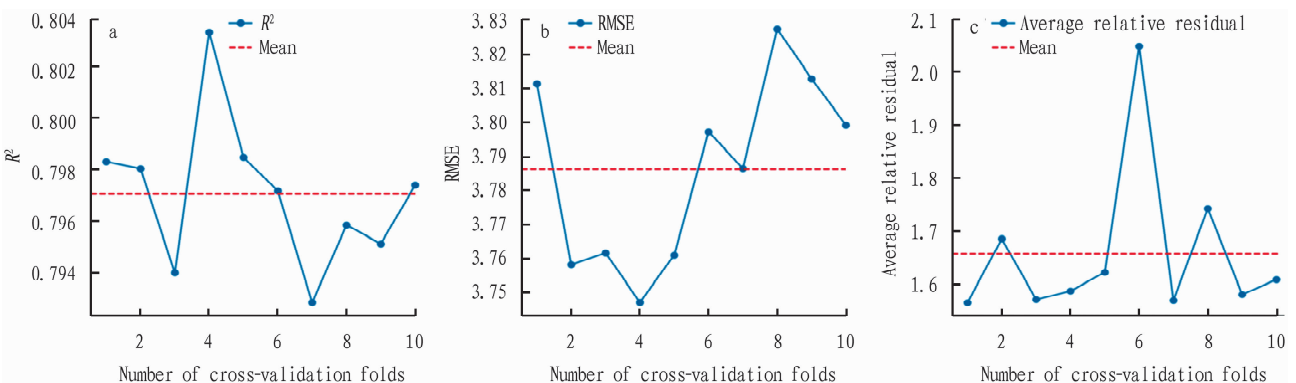
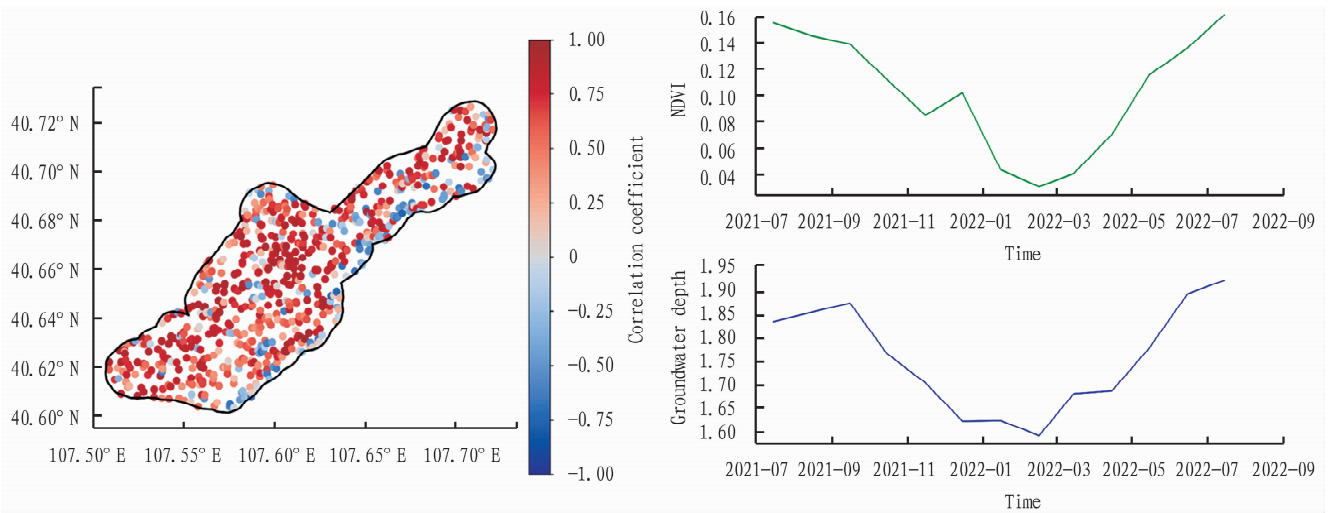
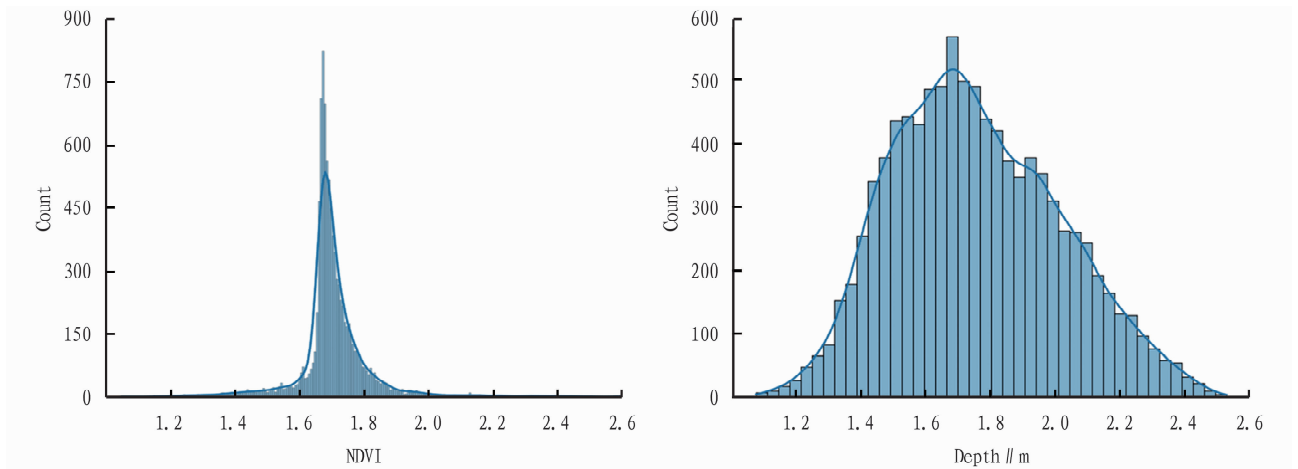


Fig.8 Cross-validation results under three tests



**Fig. 9** Spatial distribution of the correlation between NDVI and groundwater depth and their changing trends



**Fig. 10** Distribution of NDVI and groundwater depth

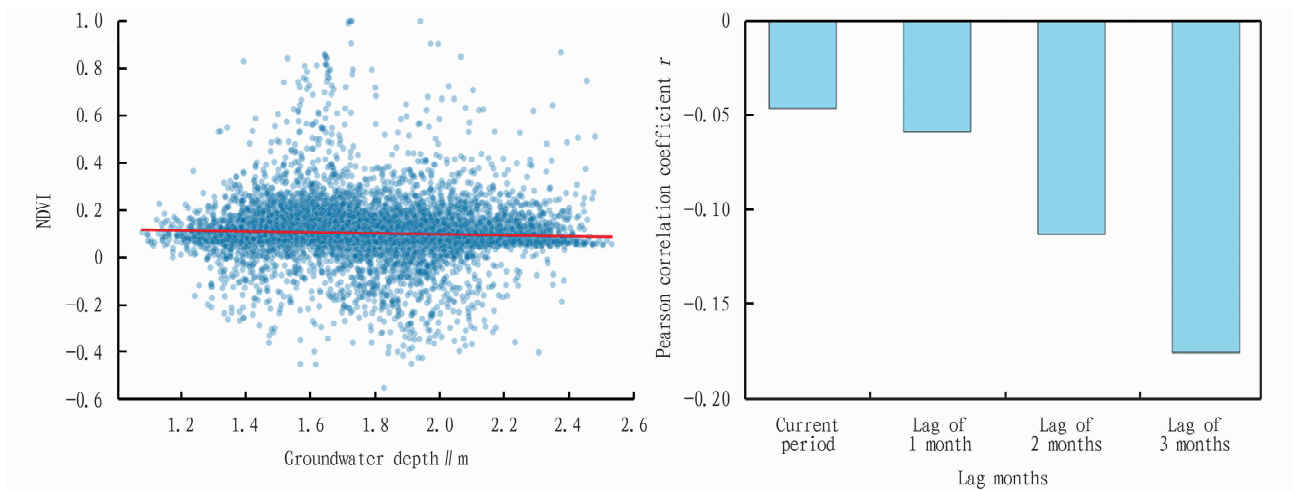


**Fig. 11** Correlation coefficient and lag correlation between NDVI and groundwater depth

type); red points (high values) represent a very chaotic land type sequence, with high uncertainty (mixed land types different in various years). The experimental area is located in the desert and its edge where a large area of bare soil remains unchanged for a long

time, so blue points are concentrated on the left side, exerting the influence contribution of negative values, which better demonstrates the varying effects of transformation of entropy values in different regions.

Dominant duration is similar to stability. Blue points (low values) mean that the duration of the dominant land type was very short. Red points (high values) indicate that the duration of the dominant land type was very long. The presented effect shows that the duration of the dominant land type was short, but the change was positive. Due to the restoration of ecological engineering in recent years, the greening effect has been remarkable, but the process is still just beginning.

As shown in Fig. 8, the  $R^2$  of the random forest model for the trajectory characteristics of land use changes was 0.7964. Here,  $R^2$  (coefficient of determination) measures the extent to which the model explains the changes in NDVI trends, with a range of 0–1. The results indicate that the random forest model based on the trajectory characteristics of land use changes can explain approximately 79.64% of the variation in NDVI trends, which belongs to moderate explanatory power. This implies that land use changes were an important factor influencing NDVI trends. However, nearly half of the variation was dominated by other factors not included in the model (such as climate, terrain, human activity intensity, etc.).

**2.3 Analysis of the correlation between NDVI and groundwater depth** This study aims to explore the temporal and spatial correlation and lag effect between vegetation activity (NDVI) and groundwater depth in the Kubuqi Desert. All data were unified to the WGS84 coordinate system (EPSG: 4326), and the vector boundaries of the study area were used for clipping. To eliminate the influence of dimension, the data of NDVI were converted to the standard range from -1 to 1. Finally, 749 valid sampling points were systematically generated within the study area, and a total of 9737 pairs of valid data of NDVI and groundwater depth were obtained for analysis. The distribution map and the time trend charts over 13 months (Fig. 9) show that they decreased in winter and increased significantly in spring and summer. At the same time, from the distribution of data points in Fig. 10 (NDVI and groundwater depth), it can be known that the groundwater depth ranged from 1.4 to 2 m, and NDVI was between 0 and 0.2 at most points in the experimental area.

Based on the data of groundwater depth and NDVI in 13 months, the Pearson correlation coefficient (Fig. 11) was calculated by using the Python method, namely -0.0464 ( $p < 0.0001$ ), indicating that there was a very weak negative correlation between NDVI and groundwater depth overall, and the correlation was statistically significant. The Spearman correlation coefficient was -0.1077 ( $p < 0.0001$ ), slightly higher than the Pearson coefficient, suggesting that the monotonic trend between the variables was slightly more obvious, but it was still a weak negative correlation.

The lag correlation between NDVI and groundwater depth was also analyzed. If there was a lag of 1 month, the Pearson correlation coefficient was -0.0590 ( $p < 0.0001$ ); if there was a lag of 2 and 3 months, the Pearson correlation coefficient was -0.1130 ( $p < 0.0001$ ) and -0.1763 ( $p < 0.0001$ ), respectively.

### 3 Discussion and problems

**The universality of vegetation improvement:** The annual average slope of NDVI in the study area was 0.006, and the median was 0.003. Moreover, the annual average growth of more than 50% of the pixels was no less than 0.003, indicating that the improvement of vegetation coverage was widespread, and the ecological condition generally improved from 2017 to 2024. In terms of significant trends, there was a significant upward trend (dominant type) in 60.93% of the pixels, confirming the effectiveness of ecological protection/repair measures; only 6.55% of the pixels showed a significant decrease, revealing that the areas with significant degradation were concentrated in a limited range, and the risk of ecological degradation was low. For the driving force of spatial heterogeneity, extreme improvement areas (slope  $> 0.05$ ) might be related to vegetation restoration projects (such as floodwater diversion project); extreme degradation areas (slope  $< -0.03$ ) might be affected by human activities (excessive development) or natural factors (drought), and targeted intervention is needed. There was a significant trend (medium reliability) in 67.56% of the pixels, and trend signals were clear, laying the foundation for subsequent analysis of driving factors; the average slope of the areas with significant changes (0.009) was higher than the overall, indicating that the ecological effect of significantly improved areas was more prominent.

From the perspective of the entire study area, when groundwater depth increased, there was a slight downward trend in NDVI, but the correlation was relatively weak. Moreover, there was a weak negative correlation between NDVI and groundwater depth in the study area, indicating that the direct impact of groundwater depth on vegetation growth (reflected by NDVI) was limited, and it may be dominated by other factors (such as precipitation, soil properties, etc.). At the same time, the negative correlation gradually strengthened with the extension of the lag time, and was statistically significant. This shows that the change in groundwater depth had a time lag effect on NDVI, and the impact was more obvious after a delay of 3 months (that is, after changes in groundwater depth, the response of NDVI was more significant 3 months later). The negative correlation also strengthened with the lag time (1–3 months), suggesting that the impact of changes in groundwater depth on vegetation had a delay, which might be related to the cycle of vegetation growth (such as root response, phenological period, etc.).

In the analysis of the correlation between NDVI and groundwater depth, 35.10% of reliable pixels were retained to effectively avoid interference such as movement of sand dunes and classification uncertainty in the desert environment, provide a high-quality data foundation for the analysis of the relationship between land use and NDVI, and ensure the reliability of the results.

In terms of model explanatory power, the  $R^2$  value of the random forest model was 0.7964 (moderate explanatory power), indicating that land use changes were an important factor affecting NDVI trends. However, 20% of the variation came from factors

not included in the model (such as climate and terrain), suggesting that subsequent studies should combine multiple factors to deepen the research on the driving mechanism. The average residual was close to 0, proving that the model had no systematic bias, and the prediction direction was reliable. However, the relative residual of only 6.71% of the regions was less than 5%, indicating that the "precise explanatory power" of land use trajectories for NDVI trends was weak in most areas. This may be due to the complexity of the trajectories (such as frequent changes) or the stronger interference of NDVI by other factors. Therefore, feature selection optimization or variable supplementation is required.

The proportion of highly correlated areas was 79.22%, indicating that NDVI changes in most areas were mainly driven by land use changes, confirming the core role of land use regulation (such as ecological engineering) in the improvement of desert vegetation. The remaining non-highly correlated areas suggest that attention should be paid to the impact of other factors such as precipitation and policies on vegetation. According to the practical guidance of SHAP features, the negative contributions (bare land, buildings) and positive contributions (forests, grasslands) of the initial/final class, and dominant class clarified the rule that "vegetation-type class promoted NDVI growth", providing a direct basis for optimizing land types (such as reducing bare land and increasing vegetation coverage) in desert ecological restoration. The contribution of location factors was not significant, indicating that the influence of uniformity of the terrain on vegetation changes in the study area can be temporarily not given priority consideration.

Although this paper has conducted a comprehensive and detailed study, it still has the following issues.

(1) Based on the time series data of NDVI in the study area from 2017 to 2024, the change trends of NDVI were analyzed. However, the  $R^2$  value of the XGBoost model for the trajectory characteristics of land use changes was 0.5107, but nearly half of the variation was still dominated by other factors not included in the model (such as climate, terrain, human activity intensity, *etc.*). Due to the lack of data from nearby meteorological stations, it is impossible to comprehensively consider the influence of factors such as temperature and precipitation.

(2) The data of land use only contained the annual average data, and lacks more detailed monthly data of vegetation coverage and precise positioning of land use types, so there is still room for improvement in calculating the changes of land use transfer and establishing the model between land use transfer and NDVI changes.

(3) The limitation of the distance between the individual points of groundwater depth in the experimental area leads to a certain error in the map of groundwater depth simulated by the technology. This may greatly affect the accuracy of correlation calculation. Therefore, more densely distributed groundwater depth points and more data of water quality at groundwater points will be beneficial for better analyzing the hydrological change process in the complex area.

(4) Initially, an attempt was made to generate a continuous correlation distribution surface using spatial interpolation methods (such as Kriging). However, the Pearson correlation coefficient, as a statistical quantity, may not possess strict geostatistical characteristics (such as intrinsic stationarity) in space, and direct interpolation might lead to misleading smoothing effects. Therefore, for the sake of rigor, this study mainly conducted spatial pattern analysis based on the calculation results of discrete sampling points, and revealed the spatial heterogeneity of the relationship between NDVI and groundwater depth by analyzing its statistical distribution characteristics and the temporal comparison of typical areas.

## 4 Conclusions

(1) During the research period, vegetation activity was improved significantly on the whole. 60.93% of the areas exhibited a significant greening trend, while there was vegetation degradation in only 6.55% of the areas.

(2) The trajectory characteristics of land use changes could explain approximately 51.07% of the variation in NDVI trends. However, its driving effect had significant spatial heterogeneity, and the area of the core driving zone accounted for 17.95%.

(3) The  $R^2$  value of the random forest model for the trajectory characteristics of land use changes was 0.7964, that is, it can explain approximately 79.64% of the variation in NDVI trends, belonging to moderate explanatory power. It reveals that land use changes were an important factor affecting NDVI trends, but about 20% of the variation was dominated by other factors not included in the model. The strongly correlated areas accounted for 79.22%.

(4) Groundwater depth was weakly negatively correlated with NDVI as a whole ( $r = -0.0464$ ), but there was a significant lag effect. When there was a lag of 3 months, the correlation coefficient increased to  $-0.1763$ .

## References

- [1] WANG RK, WANG J, ZHAO ZB, *et al.* Temporal and spatial variation analysis of vegetation coverage in Tianshui City based on MOD13Q1 data [J]. *Remote Sensing Technology and Application*, 2024, 39(4): 987 – 999.
- [2] WANG R, YANG GJ. Evaluation of ecological benefit of combating desertification in east edge of Hobq Desert [J]. *Bulletin of Soil and Water Conservation*, 2018, 38(5): 174 – 179, 188.
- [3] MU SJ, LI JL, CHEN YZ, *et al.* Spatial differences of variations of vegetation coverage in Inner Mongolia during 2001 – 2010 [J]. *Acta Geographica Sinica*, 2012, 67(9): 1255 – 1268.
- [4] XUE ZQ, GONG B, WAN L, *et al.* Analyses of variations of the Ejina Oasis and relevant factors in the downstream of the Heihe River, Northwest China [J]. *Earth Science Frontiers*, 2006(1): 48 – 51.
- [5] YANG XL, DING WK, ZHOU H, *et al.* Normalized difference vegetation index change and its driving factors in Shiyang River Basin [J]. *Arid Land Geography*, 2024, 47(10): 1735 – 1744.
- [6] SHANG X, HE ZG, ZHANG TH. Spatial and temporal variations and the driving mechanism of the enhanced vegetation index [J]. *Journal of Forest and Environment*, 2020, 40(5): 478 – 485.

- [7] TU J, ZHOU XL, WANG SS. Study on spatiotemporal changes of fractional vegetation cover in Baotou City based on NDVI in the past 20 years [J]. *Grassland and Turf*, 2024, 44(4): 121–132.
- [8] HAN HZ, HE ZJ, CHEN C, *et al.* Analysis on the spatio-temporal variation and influencing factors of net primary productivity of vegetation in the ecological region of the Yellow River basin from 2001 to 2022[J]. *Environmental Ecology*, 2024, 6(10): 56–67.
- [9] LU JK, LIU DF, LIU H, *et al.* Multiple linear regression study of vegetation index and meteorological factors at the pixel scale[J]. *Journal of North China University of Water Resources and Electric Power: Natural Science Edition*, 2020, 41(3): 14–24.
- [10] WANG H, LI XB, LI X, *et al.* The variability of vegetation growing season in the northern China based on NOAA NDVI and MSAVI from 1982 to 1999[J]. *Acta Ecologica Sinica*, 2007(2): 504–515.
- [11] YANG Y, HE RZ, TIAN GX, *et al.* Plant phenology monitoring of Zhengzhou area based on MODIS NDVI data[J]. *Journal of Southwest Forestry University: Natural Sciences*, 2018, 38(2): 111–116.
- [12] FAN DQ, ZHAO XX, ZHENG ZT. Phenology of leymus chinensis steppe in Inner Mongolia and its response to climate changes[J]. *Geography and Geo-Information Science*, 2016, 32(6): 81–86.
- [13] SEN PK. Estimates of the regression coefficient based on Kendall's tau [J]. *Journal of the American Statistical Association*, 1968, 63(324), 1379–1389.
- [14] MANN HB. Nonparametric tests against trend [J]. *Econometrica*, 1945, 13(3): 245–259.
- [15] JIANG ZW, YANG ZB, YANG Q, *et al.* Temporal and spatial variation of vegetation cover in Kubuqi Desert from 2000 to 2022 and its driving factors[J]. *Journal of Desert Research*, 2025(5): 1–10.
- [16] ZHANG XY, XI JX, YE ZH, *et al.* Relationship between vegetation community characteristics and ecological threshold of groundwater level in groundwater dependent ecosystems(GDEs)[J]. *Research of Environmental Sciences*, 2025(6): 1312–1323.
- [17] ZHANG JY. Research on the spatiotemporal variability of groundwater level and vegetation index (NDVI) in the plain area of Hebei Province [J]. *Technical Supervision in Water Resources*, 2025(3): 42–44.
- [18] PEARSON K. Notes on regression and inheritance in the case of two parents[J]. *Proceedings of the Royal Society of London*, 1895, 58: 240–242.
- [19] ROUSE JW, HAAS RH, SCHELL JA, *et al.* Monitoring vegetation systems in the Great Plains with ERTS [J]. *NASA Special Publication*, 1974, 351: 309–313.
- [20] HOLBEN BN. Characteristics of maximum-value composite images from temporal AVHRR data [J]. *International Journal of Remote Sensing*, 1986, 7(11): 1417–1434.
- [21] CLEVELAND RB, CLEVELAND WS, MCRAE JE, *et al.* STL: A seasonal-trend decomposition procedure based on LOESS [J]. *Journal of Official Statistics*, 1990, 6(1): 3–73.
- [22] FERNANDES R, LEBLANC SG. Parametric (modified least squares) and non-parametric (Theil-Sen) linear regressions for predicting biophysical parameters in the presence of measurement errors[J]. *Remote Sensing of Environment*, 2005, 95(3): 303–316.
- [23] KENDALL MG. Rank correlation methods (4<sup>th</sup> edition) [M]. Charles Griffin, London, 1975.
- [24] BREIMAN L. Random forests[J]. *Machine Learning*, 2001, 45(1): 5–32.
- [25] RODRIGUEZ-GALIANO VF, GHIMIRE B, ROGAN J, *et al.* An assessment of the effectiveness of a random forest classifier for land-cover classification[J]. *ISPRS Journal of Photogrammetry and Remote Sensing*, 2012, 67: 93–104.
- [26] STONE M. Cross-validated choice and assessment of statistical predictions[J]. *Journal of the Royal Statistical Society: Series B (Methodological)*, 1974, 36(2), 111–133.
- [27] GEISSER S. The predictive sample reuse method with applications[J]. *Journal of the American Statistical Association*, 1975, 70(350): 320–328.
- [28] LUNDBERG SM, LEE SI. A unified approach to interpreting model predictions[J]. *Advances in Neural Information Processing Systems*, 2017, 30.

## About the Databases of Meteorological and Environmental Research

The journal of Meteorological and Environmental Research [ISSN: 2152–3940] has been included and stored by the following famous databases: CA, CABI, CSA, EBSCO, UPD, AGRIS, EA, Chinese Science and Technology Periodical Database, and CNKI, as well as Library of Congress, United States.

CA (Chemical Abstracts) was founded in 1907, and is the most authoritative and comprehensive source for chemical information. Centre for Agriculture and Bioscience International (CABI) is a not-for-profit international agricultural information institute with headquarters in Britain. ProQuest CSA belongs to Cambridge Information Group (CIG), and it provides access to more than 100 databases published by CSA and its publishing partners. EBSCO is a large document service company with a history of more than 60 years, providing subscription and publication services of journals and documents. CNKI (China National Knowledge Infrastructure), universally acclaimed as the most valuable Chinese website, boasts the greatest information content, covering natural science, humanities and social science, engineering, periodical, doctor/master's dissertations, newspapers, books, meeting papers and other miscellaneous public information resources in China.